

# Easy-To-Use CAD Tools for Litz-Wire Winding Optimization

J. Pollock  
T. Abdallah  
C. R. Sullivan

Found in *IEEE Applied Power Electronics Conference*, Feb. 2003,  
pp. 1157–1163.

©2003 IEEE. Personal use of this material is permitted. However, permission to reprint or republish this material for advertising or promotional purposes or for creating new collective works for resale or redistribution to servers or lists, or to reuse any copyrighted component of this work in other works must be obtained from the IEEE.

# Easy-To-Use CAD Tools for Litz-Wire Winding Optimization

Jennifer D. Pollock, Tarek Abdallah and Charles R. Sullivan

jenna.pollock@dartmouth.edu

charles.r.sullivan@dartmouth.edu

http://engineering.dartmouth.edu/inductor

8000 Cummings Hall, Dartmouth College, Hanover, NH 03755, USA

**Abstract**—Existing advanced and powerful techniques for optimizing litz-wire winding designs are complex and usually require using multiple expensive software packages. A new CAD tool has been created to make advanced litz-wire design methods available to any designer through an easy-to-use web interface. The software performs two-dimensional field simulations and returns designs optimized considering cost and loss. It is shown that simple full-bobbin designs, compared to optimized choices, can result in much higher loss with almost no cost advantage or much higher cost with almost no loss advantage, whereas the optimization results provide a full range of choices providing the lowest loss at any given cost or the lowest cost at any given loss.

## I. INTRODUCTION

**W**INDING losses in magnetic components operated at high frequency in power converters can severely limit performance and prevent size and cost reductions. Litz wire can be used to reduce high-frequency losses, but design with litz wire is difficult; a poor litz-wire design can easily have higher loss than a simple solid-wire design [1], [2]. Thus, to realize the potential benefits of litz wire, it is essential to do careful design analysis.

There is a rich body of literature on litz wire analysis and optimization techniques [2]-[8]. However, the more advanced and powerful techniques that have been developed are complex enough that they do not invite use by practicing engineers for routine work. General-purpose software for analyzing electromagnetic fields using finite element analysis or other techniques is readily available from many vendors, but it has several severe limitations for litz-wire design. Firstly, analyzing the eddy currents within thousands of small strands requires orders of magnitude more memory and computation time than typical problems do, and so remains impractical on standard computers. Secondly, a numerical solution provides information about the losses in one design, but does not directly provide information on how to improve the design. Because the litz-wire user can choose from a vast array of strand sizes and numbers of strands, it is difficult to locate a good design simply by trying different possibilities.

We have created software that implements some of the most advanced and powerful recently published litz-wire design methods in easy-to-use software. The full capabilities are available in software that can be downloaded at no charge from our website, in the MATLAB programming language [9]. A version with most of the capabilities is being made available directly through a web interface. Users of this version need no software other than a web browser and can work from any platform; the calculations are performed on the web server [22].

This work was supported in part by the United States Department of Energy under grant DE-FC36-01GO1106

The method chosen for implementation is the approach in [10]. It uses the squared-field-derivative (SFD) method [11] to handle different nonsinusoidal waveforms in each winding, properly accounting for mutual resistance effects [12]. The SFD method also handles two-dimensional (2-D) or three-dimensional (3-D) field effects, by combining analytical modeling of the strand-level eddy-current loss effects with numerical calculations of the overall field shapes. In [10], the SFD method is combined with a cost analysis of litz wire [2] in order to optimize a particular flyback transformer. We have taken the method used for this example in [10] and implemented a general-purpose version of it in easy-to use software. For the convenience of the reader, the method in [10] is reviewed in detail in Appendix I. A brief overview of the method is provided in Section I-A.

Because the SFD method [11] entails the use of a numerical field solution, an easy-to-use software tool must have that capability built in. Section II describes the 1-D and 2-D field solutions that are included in both versions of our software. Section III describes the MATLAB implementation, and Section V describes the web-based version.

### A. Analysis and Optimization Approach

The SFD method is a generalized version of an approach to nonsinusoidal waveforms that has been widely used [8], [13], [14], [15]. It is based on the dependence of losses on the squared derivative of the field,  $(\frac{dB}{dt})^2$ . With a uniform field within a conducting cylinder (such as an individual strand in a litz-wire winding), instantaneous power dissipation  $P(t)$  in a wire of length  $\ell$  is given by

$$P(t) = \frac{\pi \ell d_c^4}{64 \rho_c} \left( \frac{dB}{dt} \right)^2, \quad (1)$$

where  $B$  is the flux density, assumed perpendicular to the axis of the cylinder,  $\rho_c$  is the resistivity of the wire, and  $d_c$  is its diameter [11]. The assumption of uniform field is valid when the diameter of a strand is small compared to a skin depth. For most well designed litz-wire windings, this is the case. For applications with a wide spectrum of frequencies, either because of strong high-frequency current harmonics or because of a large low-frequency or dc current component, good designs may have wire that is large compared to a skin depth for the highest frequency content. In such cases, the SFD method will be conservative; actual loss will be somewhat smaller than predicted.

Given the dependence of loss on  $(\frac{dB}{dt})^2$ , and given that  $B$  is a linear function of the current in different windings, it is possible to account for the losses resulting from these different currents

using a “dynamic loss matrix”  $\mathbf{D}$  [11]

$$P_{eddy} = \begin{bmatrix} \frac{di_1}{dt} & \frac{di_2}{dt} \end{bmatrix} \mathbf{D} \begin{bmatrix} \frac{di_1}{dt} \\ \frac{di_2}{dt} \end{bmatrix}. \quad (2)$$

The matrix  $\mathbf{D}$  is calculated, independent of current waveforms, using a series of simplified magnetostatic field simulations—one for each winding excited alone, and one for each possible pair of windings. The accuracy of the SFD method has been experimentally verified in [11].

In [10], it is shown that this method of calculating losses can be used as the basis for finding the optimal number and diameter of strands in a litz-wire winding, similar to the optimization in [2], but valid for arbitrary geometries and current waveforms. As shown in [8], it is essential to consider cost in litz-wire optimization, because the minimum-loss design, considered independent of cost, typically uses prohibitively expensive constructions with many extremely fine strands. On the other hand, simple rule-of-thumb approaches to choosing strand diameter can result in higher loss and higher cost than an optimized design [2], or even higher loss than simple single-strand windings [1]. Thus, the optimization is necessary.

As shown in [2], [10] and reviewed in the appendix, considering cost and loss results in a set of possible designs that can be plotted as in Fig. 1. Each of the designs on this curve—the optimal design frontier—gives the lowest cost at a given loss (and the lowest loss at a given cost). The designer must then choose a cost/loss tradeoff appropriate for a particular application. The optimal design frontier can be expressed in terms of a cost function  $C_m(d_c)$  which gives cost per unit mass as a function of strand diameter, its derivative  $C'_m(d_c)$ , and an eddy current loss factor  $F_e$ , analogous to the ac resistance factor  $F_r$ , but defined as the ratio of the actual winding losses  $P_w$  to the losses expected based on dc resistance,  $P_r$ , to facilitate accounting for waveforms with both ac and dc components:  $F_e = \frac{P_w}{P_r}$ . Given these definitions, the optimal design frontier can be shown to satisfy [10]

$$F_{e,CL}(d_c) = 1 + \frac{1}{1 - \frac{2C_m(d_c)}{C'_m(d_c)d_c}}. \quad (3)$$

This result can be used with (2) to solve for the other parameters of the optimal designs and find their loss, as detailed in Appendix I and in [10]. The cost function  $C_m$  may be the curve fit to manufacturers’ quotes as in [2], or a new curve-fit may be substituted to represent updated prices from a given supplier. This method has been experimentally verified in [10].

## II. MAGNETIC FIELD CALCULATIONS

In order to apply the method described in Section I-A, it is necessary to perform a set of simple magnetostatic field calculations. In [10], these calculations were performed with commercial finite-element software. The relevant field quantities were transcribed for use in the optimization. This approach is not compatible with our objective of making software that is easily available to any designer, and that is easy to use. We wished to make optimization available for users who do not have access

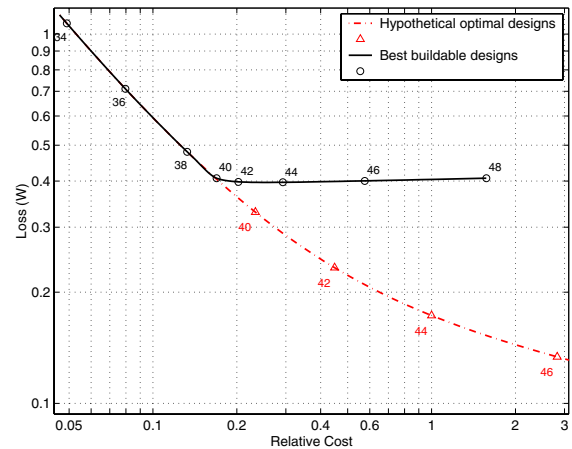


Fig. 1. An example of the optimal design frontier produced by LitzOpt. The solid line represents the best buildable designs with a circle indicating the even AWG sizes. To the left of the minimum loss design (near AWG 44), these designs provide the lowest loss at any given cost or the lowest cost for any given loss. The dash-dot curve shows the hypothetical optimal designs which ignore the space constraints imposed by the bobbin window.

to expensive finite-element software packages, and we wished to avoid the tedious process of running several different programs and transferring data to obtain a solution. Thus, we developed numerical field solutions as part of our software. The user has the option to use a simpler 1-D solution or a 2-D solution that takes into account the 2-D effects that result from air gaps in the core or unusual winding layouts.

### A. One-Dimensional Magnetic Field Calculations

For 1-D solutions, a simple MMF-diagram approach [16] is used to evaluate the field. The quantities needed for the SFD method (the average of  $B^2$  over each winding) have been calculated analytically for a variety of different configurations which may be selected by the user.

### B. Two-Dimensional Magnetic Field Calculations

The method of images [17] is well suited to analysis of the magnetic field in a rectangular winding window of an ungapped, high-permeability core, considered in two dimensions [18], [19]. Since each wall of the window can be replaced by an image of the rest of the geometry, the effect of the core can be modeled by an infinite set of images of the windings, similar to the images visible in a room with mirrors on all four walls. The effect of the images on the field declines with distance, and we find that a five-by-five grid of images, as shown in Fig. 2, is typically sufficient for better than 0.05% accuracy.

With the effect of the core removed by imaging, the problem is reduced to that of finding the field due to a collection of currents. We address only the case of rectangular current distributions, as in typical winding shapes, for which we use the closed-form solution for the field detailed in Appendix II [17], [18].

As derived in [19], the same approach can be used to calculate the field with a gapped core by replacing the gap with a ribbon of current on the inside surface of the core. The total current in

all gap ribbons is set equal and opposite to the total current in all the windings, such that the net current through the window is zero (as it must be with the assumption of an infinite-permeability core).

To find the average value of  $B^2$  over a given winding, as required for the SFD method, the squared field is integrated over each winding, using a simple rectangular midpoint numerical integration approach. Even with this crude integration method, the time required to achieve an accurate solution is competitive with commercial finite element packages: under five seconds for 0.05% accuracy for a simple gapped inductor on a 1 GHz Pentium III machine. The accuracy quoted above is as compared to a finite-element analysis program running the same 2-D solution using a very fine mesh. Errors resulting from the use of a 2-D solution to represent a 3-D device will generally be more significant [20], [21].

### III. MATLAB IMPLEMENTATION

The method as described in Sections I-A and II has been implemented in a MATLAB program called LitzOpt that may be freely downloaded from our website [22]. The program's graphical user interface prompts the user for some basic data, and then creates a blank data file with fields for the necessary geometry and current-waveform data. The program performs field calculations as described in Section II and implements the optimization approach as described in Section I-A and Appendix I. The user is provided with a plot of the optimal design frontier, such as the example in Fig. 1, and a table of wire size, number of strands, loss, and relative cost for each recommended design. Each of the designs listed or shown in Fig. 1 provides minimum cost for a given loss or minimum loss for a given cost. The user can then select a design according to the cost/loss tradeoff appropriate for the application under consideration.

The program has the ability to automatically allocate space for the windings in the winding window using a standard layered winding configuration. The height of each winding is determined by

$$h_i = \left[ \frac{N_i I_{rms,i}}{\sum N_i I_{rms,i}} \right] h_b, \quad (4)$$

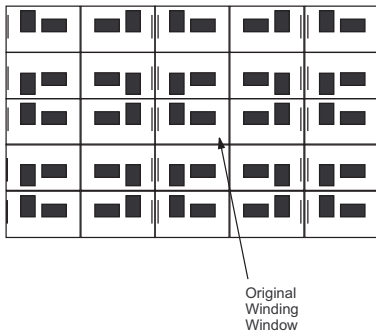


Fig. 2. Applying the method of images results in replacing a high-permeability core with an infinite number of images of the windings in the original winding window. A system of 24 images plus the original winding window, as shown here, is found to give better than 0.05% accuracy for typical examples. The ribbon at the left of the window is used to model the effect of a gap (see text); in practice it has zero thickness and is all the way at the edge of the window.

where  $h_i$  is the height of each winding,  $N_i$  is the number of turns in that winding,  $I_{rms,i}$  is the RMS current in the winding and  $h_b$  is the height of the bobbin window. This allocation would be the optimum based only on considerations of DC resistance and ignoring the effect of winding position on turn length. Using this feature is convenient for the designer not only because it automatically calculates a good allocation of winding space, but also because it reduces the amount of data that must be entered into the program. The user also has the option to fully specify any desired winding configuration.

To determine what possible stranding designs would fit on the bobbin, the program uses the maximum achievable packing factor specified by the user, which indicates the maximum density of wire that can be obtained in manufacturing the device. The packing factor,  $F_p$ , is the ratio of actual achievable wire packing relative to the perfect square packing of cylinders, and is defined as

$$F_p = \frac{A_{wi}}{A_{available}} \frac{4}{\pi}, \quad (5)$$

where  $A_{wi}$  is the total cross-sectional area of wire including copper and insulation but not air space between strands and  $A_{available}$  is the area available for the winding and is equal to the height of the bobbin window times the breadth of the bobbin window. The default value for  $F_p$  is 0.6, but typical values range from 0.3 to 0.9 [23]. The determination of the total cross-sectional area of wire with insulation is taken from [2] and depends on the size of the wire and insulation build selected by the user.

The program first calculates an optimal design ignoring the bobbin space constraint. It then checks to see if each optimal design will fit in the available winding area. If a design fits in the winding area, then the design is called the best buildable design. If an optimal design does not fit, the program adjusts the stranding, resulting in a full-bobbin design that is as close as possible to the original calculated optimum. The cost and loss are recalculated for each new design.

A typical output is shown in Fig. 1, but more detail is shown in Fig. 3. The lowest curve shows the original calculated optimal designs. For designs to the left of the AWG 38 design, the optimal designs fit on the bobbin. For AWG 40 designs and those to the right of this point, the optimal designs do not fit, and a full bobbin is chosen instead. Fig. 3 also shows the result of selecting a full bobbin in the region where the optimal design does not fill the bobbin.

### IV. DISCUSSION OF OPTIMIZATION RESULTS

The results in Fig. 3 are for one example design. Depending on the size of the winding window and other parameters, the full-bobbin constraints may be more or less important. With a sufficiently large winding window, all of the optimal designs as originally calculated without considering the bobbin constraint will be buildable, and the designer may select from a wide range of cost/loss tradeoffs along a smooth curve, the lowest curve in Fig. 3, solid on the left and dash-dot on the right. The best choice along that curve will depend on the relative importance of initial cost and loss, as discussed in [2].

In most cases, however, the original optimal curve will become hypothetical at some point where the bobbin becomes full, as happens between AWG 38 and AWG 40 in Fig. 3. Beyond this critical point, a full bobbin always gives the lowest loss. Using finer wire continues to reduce eddy-current loss, but dc resistance starts to increase because insulation constitutes a larger fraction of the wire cross section for smaller diameter wire. Thus, there is a tradeoff between dc resistance and eddy-current loss which, in Fig. 3, first results in the small decrease in loss between AWG 40 and AWG 44, and then results in a slight increase in loss beyond AWG 44. The point giving minimum loss, near AWG 44 in this case, was found analytically for simple geometries in [8]. However, [8] did not include an analysis of cost. With the cost analysis included, we see in Fig. 3 that the minimum loss point analyzed in [8] is not very interesting in practice, because, from where the optimal designs first fill the bobbin to the minimum loss design (AWG 40 to AWG 44 in Fig. 3), the loss reduction is tiny (3% in this case) while the cost increase is large (a factor of two in this case).

Because designs to the right of the critical point where optimal designs first fill the bobbin have small loss reductions for large cost increases, the practical designs that should be considered are usually just the optimal designs that do not fill the bobbin, up to the point where they first fill the bobbin (AWG 34 through 40 in the example shown in Fig. 3.) It is likely that in many cases, the first optimal design that fills the bobbin will be the best choice, because up to that point, the curve in Fig. 3 is steep—large loss reductions are possible with small increases in cost. However, one must be careful not to condense this conclusion to the idea that a full bobbin is optimal. The curve of full-bobbin designs is almost vertical to the left of the critical point, showing losses skyrocketing with almost no savings in cost. Thus, these full-bobbin designs are very poor choices that have higher cost and loss than the alternatives without the bobbin filled.

In Fig. 3, one might choose designs with an underfilled bobbin,

to the left of the critical point (AWG 40), in order to save on cost if the loss was not critical. In other situations, the critical point can be even further to the right, making underfilled bobbins optimal for even more wire sizes. Even without the full-bobbin constraint, the optimal design curve flattens out significantly beyond AWG 44 wire, as a result of the increased cost of manufacturing finer strands [2]. Thus, in situations where the critical point is further to the right, choosing an underfilled bobbin becomes more attractive.

Although we can conclude that an underfilled bobbin will often be the optimal winding design when cost is considered, that is no longer the case if we allow varying the core geometry as well. Given a design with an underfilled bobbin, the core window height could be shrunk with no penalty in winding loss; this would provide a reduction in core loss and in cost of core material. However, for most designs, it is advantageous to stick to standard core geometries, and such modifications are not available options.

We conclude that underfilled bobbins will often be the best practical designs, and that in that region the optimization provides important guidance to selecting a better design than the disastrous full-bobbin designs to the left of the critical point in Fig. 3. The full-bobbin design at the critical point will also often be the best design in practice, because it is the last point at which loss reductions can be obtained for a reasonable cost increase. Again, the optimization is critical in performing this design—full bobbins with smaller strands provide almost no loss reduction but greatly increase cost, whereas full bobbins with larger strands provide almost no cost reduction, but produce a rapid increase in loss.

## V. WEB INTERFACE

In the web-based version, the same MATLAB program runs in MATLAB on the web server. A web interface system [24] extracts the data from the html forms submitted by the designer and delivers the data to LitzOpt. The program calculates the optimal design frontier as described in Section III and inserts the results into a web page that is sent back to the user.

The user is guided through the data entry process with a web-based user interface as shown in Fig. 4. The required data comprises the following: number of windings; number of turns, size, and location of each winding; number of gaps, gap locations and lengths; dimensions of the core and bobbin window; maximum achievable packing factor; and winding insulation build.

Current excitation data is entered as either a piecewise-linear waveform or as frequency, amplitude, and phase of a sinusoidal waveform for each winding. The web-based implementation allows a piece-wise linear current waveform to be broken into 10 time segments for up to 5 different windings; the full MATLAB version allows any number of windings and any number of time segments. The user is able to view the current waveform created from the data entered to confirm that it is as intended.

The field calculation and optimization in the web-based version is identical to the MATLAB version. Again, the user is provided

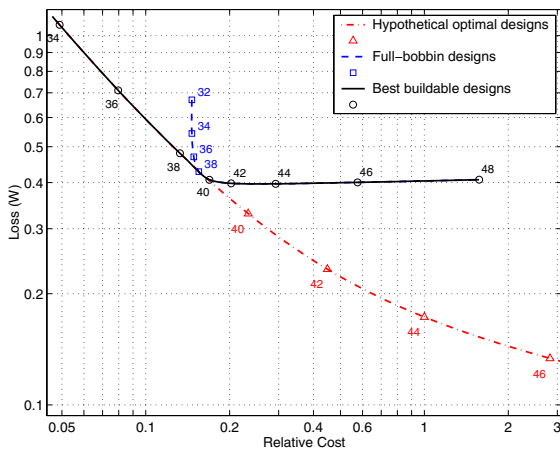
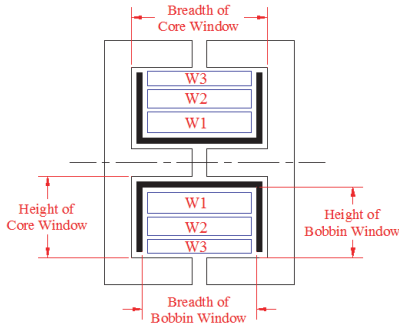


Fig. 3. Cost vs. loss for optimal and full-bobbin designs, for the same example as in Fig. 1. The solid black line shows the best buildable designs. The dash-dot line below this shows optimal designs that will not fit in the winding window with the given packing factor. The dashed line above the best buildable design curve shows full bobbin designs that are not optimal.

Dartmouth Magnetic Component and Power Electronics Research		
<b>LitzOpt 2D Data Entry</b>		
<b>Directions:</b> Enter information requested to optimize a magnetic component with a piece-wise linear waveform. For details on each variable, click on the name.		



Variable	Value	Units
Temperature	25	Degrees C
Maximum Achievable Packing Factor	.5	
bw - Breadth of Core Window	0	mm
h - Height of Core Window	0	mm
bb - Breadth of Bobbin Window	0	mm
hb - Height of Bobbin Window	0	mm
Number of Windings	0	
Number of Time Segments	0	
Gap Length	0	mm
<b>Location of Gap</b>		
<input checked="" type="radio"/> Center Leg Gapped <input type="radio"/> Both Outer Legs Gapped <input type="radio"/> No Gaps <input type="radio"/> All Legs Gapped		
<b>Winding Insulation Build</b>		
<input checked="" type="radio"/> Single Build Insulation <input type="radio"/> Heavy Build Insulation		

Winding Information						
		W1	W2	W3	W4	W5
Number of Turns		0	0	0	0	0
Average Length of a Turn (mm)		0	0	0	0	0
Time Segments	Current					
	Microseconds	at I (A)				
dt1	Start of dt1	0	0	0	0	0
	End of dt1	0	0	0	0	0
dt2	Start of dt2	0	0	0	0	0
	End of dt2	0	0	0	0	0
dt3	Start of dt3	0	0	0	0	0
	End of dt3	0	0	0	0	0
dt4	Start of dt4	0	0	0	0	0
	End of dt4	0	0	0	0	0
dt5	Start of dt5	0	0	0	0	0
	End of dt5	0	0	0	0	0
dt6	Start of dt6	0	0	0	0	0
	End of dt6	0	0	0	0	0
dt7	Start of dt7	0	0	0	0	0
	End of dt7	0	0	0	0	0
dt8	Start of dt8	0	0	0	0	0
	End of dt8	0	0	0	0	0
dt9	Start of dt9	0	0	0	0	0
	End of dt9	0	0	0	0	0
dt10	Start of dt10	0	0	0	0	0
	End of dt10	0	0	0	0	0

Fig. 4. Web-based data entry: The 2-D data-entry page for a piecewise current waveform. After entering the current data, the user is provided with a waveform plot for verification.

with a table of possible recommended designs and a plot as in Fig. 1, this time in the medium of a web page. The user can then select a cost/loss tradeoff appropriate to the application.

## VI. CONCLUSION

New software has been developed to make state-of-the-art litz-wire design methods easily available to any magnetics designer. The software is available in two forms: a program that can be freely downloaded and run in MATLAB, and a web-based system that runs on the server and may be used from any machine. The software includes 2-D field analysis based on the method of images, and can provide 0.05% accuracy field solutions in seconds. These field solutions are used with the experimentally-verified methods in [11] and [10] to develop a set of choices for number of litz-wire strands and strand diameter, each of which provides minimum loss for a given cost or minimum cost for a given loss.

A comparison of simple full-bobbin designs to the optimal options shows the importance of optimization. Although some optimal designs use a full bobbin, most full-bobbin designs result in much higher loss with almost no cost advantage or much higher cost with almost no loss advantage. Having easy-to-use optimization tools is thus critical to economical and efficient application of litz wire.

## VII. ACKNOWLEDGEMENTS

Thanks to Weyman Lundquist of West Coast Magnetics and Dj Merrill of Thayer School of Engineering, Dartmouth College.

## APPENDIX I

### REVIEW OF COST/LOSS OPTIMIZATION METHOD

The analysis of litz wire cost and loss for arbitrary waveforms and geometries developed in [10] and implemented in the software described in this paper is based on extending the 1-D method for sinusoidal waveforms in [2]. The method in [2] is based on the ac resistance factor,  $F_r = R_{ac}/R_{dc}$ , which can, for the simple configurations addressed in [2], be expressed:

$$F_r = 1 + \frac{k\pi^2\omega^2\mu_0^2N^2n^2d_c^6}{768\rho_c^2b_c^2} \quad (6)$$

where  $\omega$  is the radian frequency of a sinusoidal current,  $n$  is the number of litz-wire strands,  $N$  is the number of turns,  $d_c$  is the diameter of the conductor in each strand,  $\rho_c$  is the resistivity of the conductor,  $b_c$  is the breadth of the window area of the core, and  $k$  is a factor accounting for field distribution in multi-winding transformers [23], [8]. To apply a similar approach to more general situations, [10] introduces a factor  $F_e$ , analogous to  $F_r$ , but defined as the ratio of the actual losses to the losses expected based on dc resistance:

$$F_e = \frac{P_w}{P_r} = 1 + \frac{P_e}{P_r} \quad (7)$$

where  $P_w$  is the total power lost in the winding,  $P_e$  is the power lost due to eddy currents,  $P_r$  is the loss expected based on dc resistance ( $P_r = I_{rms}^2 R_{dc}$ ). Without dc current or mutual resistance effects,  $F_e$  and  $F_r$  are equal; (6) is also an expression for  $F_e$  in the simple situations analyzed in [2]. Equation (6) can be rewritten in terms of the cross-sectional area of a strand ( $A_s = d_c^2 \pi/4$ ), as

$$F_e = 1 + k_\ell n^2 A_s^3 \quad (8)$$



where  $k_\ell$  represents constant terms of (6) lumped together. The analysis in [2] can be applied to optimize cost and loss whenever loss can be expressed in the same form as (8). As shown in [10] this includes the losses calculated by the SFD method [11].

To put the losses calculated by the SFD method in the form of (8), [10] writes the power loss due to eddy currents as  $P_e = k_1 n A_s^2$  and the resistive power loss as  $P_r = k_2 (n A_s)^{-1}$ , lumping the constants other than  $n$  and  $A_s$  into  $k_1$  and  $k_2$ . This results in

$$F_e = 1 + \frac{k_1 n A_s^2}{\frac{k_2}{n A_s}} \quad (9)$$

After simplification, (9) yields (8) with  $k_\ell = k_1/k_2$ . This shows that the cost/loss optimization method discussed in [2] can be applied to more general situations analyzed by the SFD method [11]. In order to implement the optimization a value for  $k_\ell$  must be calculated.

To find  $k_\ell$ , one could equate (8) and (7); solving for  $k_\ell$  yields

$$k_\ell = \frac{P_e}{P_r n_j^2 A_s^3}. \quad (10)$$

This expression could be used to calculate  $k_\ell$  from a completed design. However, it is possible, and more often useful, to calculate the optimal designs without any initial design to work from. In the next section, we present the calculation of  $k_\ell$  developed in [10] that is independent of any particular initial design.

#### A. Evaluation of $k_\ell$

As shown in [11],  $P_e$  can be found by defining a dynamic resistance matrix,  $\mathbf{D}$ , containing transformer characteristics. In the pursuit of finding  $k_\ell$  for a particular winding ( $k_{\ell,j}$ ) independent of its stranding parameters, [10] defines a modified dynamic resistance matrix with the stranding parameters  $n$  and  $A_s$  factored out:  $\tilde{\mathbf{D}} = \frac{\mathbf{D}}{n_j A_{s,j}^2}$ , and uses only the portion of  $\tilde{\mathbf{D}}$  associated with losses in the winding of interest:  $\tilde{\mathbf{D}}_j$ . Reference [11] calculates  $\mathbf{D}$  in terms of a loss coefficient,  $\gamma_j$  for each winding  $j$ , which accounts for the influence of the stranding parameters on  $\mathbf{D}$ . To remove that influence, [10] defines a modified loss coefficient:

$$\tilde{\gamma}_j = \frac{\gamma_j}{n_j A_{s,j}^2} = \frac{\ell_{w,j}}{4\pi\rho_c}. \quad (11)$$

Here,  $\ell_w$  is the length of the entire winding, equal to the average length of a turn multiplied by the number of turns:  $\ell_w N \ell_t$ .

One can calculate  $\mathbf{D}_j$  from  $\tilde{\gamma}_j$  and from the results of magnetostatic field calculations of the field due to unit current in each winding [10]. The calculation of  $\tilde{\mathbf{D}}$  is expressed in terms of the field due to unit current in winding  $m$ ,  $\hat{\mathbf{B}}_m$ , as

$$\tilde{\mathbf{D}}_j = \tilde{\gamma}_j \langle \left[ \begin{array}{cc} |\hat{\mathbf{B}}_1|^2 & \hat{\mathbf{B}}_1 \cdot \hat{\mathbf{B}}_2 \\ \hat{\mathbf{B}}_2 \cdot \hat{\mathbf{B}}_1 & |\hat{\mathbf{B}}_2|^2 \end{array} \right] \rangle_j \quad (12)$$

where  $\langle \rangle_j$  signifies the spatial average over the region of the winding  $j$ . The eddy current loss in winding  $j$  can be related to the modified dynamic resistance matrix:

$$P_{e,j} = n_j A_{s,j}^2 \left[ \begin{array}{cc} \frac{di_1}{dt} & \frac{di_2}{dt} \end{array} \right] \tilde{\mathbf{D}}_j \left[ \begin{array}{c} \frac{di_1}{dt} \\ \frac{di_2}{dt} \end{array} \right]. \quad (13)$$

The resistive loss can be written

$$P_{r,j} = I_{rms,j}^2 R_{dc,j} = \frac{I_{rms,j}^2 \ell_{w,j} \rho_c}{n_j A_{s,j}}. \quad (14)$$

Now it is possible to obtain  $k_{\ell,j}$  using (10) and, as a consequence, show the independence of  $k_\ell$  with respect to the number of strands and their cross-sectional area, by dividing (13) by (14):

$$k_{\ell,j} = \frac{\left[ \begin{array}{cc} \frac{di_1}{dt} & \frac{di_2}{dt} \end{array} \right] \tilde{\mathbf{D}}_j \left[ \begin{array}{c} \frac{di_1}{dt} \\ \frac{di_2}{dt} \end{array} \right]}{I_{rms,j}^2 \ell_{w,j} \rho_c}. \quad (15)$$

#### B. Cost/Loss Optimization

With a value of  $k_\ell$  calculated, the analysis in [2] can be applied almost directly to optimize cost and loss. The analysis assumes that the cost of litz wire can be approximately described by

$$Cost = (C_0 + C_m(d_c) d_c^2 n) \ell \quad (16)$$

where  $C_0$  is a base cost per unit length associated with the bundling and serving operations,  $C_m(d_c)$  is a cost basis function proportional to the additional cost per unit mass for a given strand diameter  $d_c$ ,  $n$  is the number of strands, and  $\ell$  is the length of the wire. For the purpose of optimization with a fixed winding length, we can ignore  $C_0$ , and consider only the cost variation which is proportional to  $C_m(d_c) d_c^2 n$ . In [2], a curve fit to manufacturers' data finds a function that can be used to approximate  $C_m(d_c)$

$$C_m(d_c) = 1 + \frac{k_1}{d_c^6} + \frac{k_2}{d_c^2} \quad (17)$$

where  $d_c$  is in meters,  $k_1 = 1.1 \times 10^{-26} \text{ m}^6$ ,  $k_2 = 2 \times 10^{-9} \text{ m}^2$ , and  $C_m(d_c)$  is normalized to a value of one for large  $d_c$ .

A solution for the minimum cost at any loss and vice versa is found in [2]. The solution assumes (16) but, because it can be expressed in terms of  $C_m(d_c)$ , is valid either for the particular cost function (17), or for any other  $C_m(d_c)$  that might be substituted to represent cost for a particular manufacturer or cost reduced by a new manufacturing technology. One convenient way to express the result is in terms of the optimum eddy current loss factor  $F_e$ ,

$$F_{e,CL}(d_c) = 1 + \frac{1}{1 - \frac{2C_m(d_c)}{C_m(d_c)d_c}} \quad (18)$$

Given an optimal value of  $F_e$  for a given strand size,  $F_{e,CL}$ , the number of strands can be found from (8), and then the cost can be found from (16) and the total winding loss can be found from eddy loss (13) summed with resistive loss (14). If these calculations are repeated for a range of different strand sizes, a menu of choices optimized for different cost/loss tradeoffs results.

## APPENDIX II

### FIELD DUE TO A RECTANGULAR CURRENT DISTRIBUTION

The field due to a uniform rectangular distribution of current can be calculated analytically [17], [18]. Consider a rectangular distribution of current flowing perpendicular to the page, as shown in Fig. 5. At the point labeled  $A$ , the horizontal component of the field is

$$H_x = \frac{I}{8\pi ab} [(y+b)(\theta_1 - \theta_2) - (y-b)(\theta_4 - \theta_3) + (x+a) \log_e \left( \frac{r_2}{r_3} \right) - (x-a) \log_e \left( \frac{r_1}{r_4} \right)] \quad (19)$$

and the vertical component is

$$H_y = \frac{-I}{8\pi ab} [(x+a)(\theta_2 - \theta_3) - (x-a)(\theta_1 - \theta_4) + (y+b) \log_e \left( \frac{r_2}{r_1} \right) - (y-b) \log_e \left( \frac{r_3}{r_4} \right)] \quad (20)$$

where  $I$  is the total current in the rectangular region;  $x$  and  $y$  are the coordinates of the measurement point  $A$  relative to an origin at the center of the current region;  $r$  and  $\theta$  are the distances and angles from the corners of the rectangle to the measurement point  $A$ ; and  $a$  and  $b$  are the half-height and half-width of the current region. Note that for the angle differences in (20) and (19), the angles must be specified such that  $|\theta_i - \theta_j| < \pi$ .

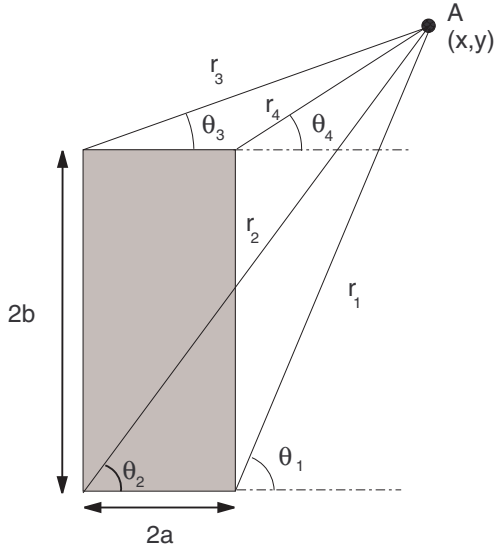


Fig. 5. Coordinates used in calculating the field (at point  $A$ ) due to a uniform, rectangular distribution of current (shaded area; current flow is perpendicular to the page).

## REFERENCES

- [1] D. Devlin, "Sorting out losses in high frequency magnetic design", *Power Electronics Technology*, May 2002.
- [2] C. R. Sullivan, "Cost-constrained selection of strand wire and number in a litz-wire transformer winding", *IEEE Transactions on Power Electronics*, vol. 16, no. 2, pp. 281–288, Mar. 2001.
- [3] B. B. Austin, "The effective resistance of inductance coils at radio frequency", *The Wireless Engineer*, vol. 11, pp. 12–16, Jan. 1934, Summary of work by S. Butterworth.
- [4] P. N. Murgatroyd, "Calculation of proximity losses in multistranded conductor bunches", *IEE Proceedings, Part A*, vol. 36, no. 3, pp. 115–120, 1989.
- [5] J. A. Ferreira, "Analytical computation of ac resistance of round and rectangular litz wire windings", *IEE Proceedings-B Electric Power Applications*, vol. 139, no. 1, pp. 21–25, Jan. 1992.
- [6] J. Schutz, J. Roudet, and A. Schellmanns, "Modeling litz wire windings", in *IEEE Industry Applications Society Thirty-Second Annual Meeting*, 1997, pp. 1190–5 vol.2.
- [7] A. W. Lotfi and F. C. Lee, "A high frequency model for litz wire for switch-mode magnetics", in *Conference Record of the 1993 IEEE Industry Applications Conference Twenty-Eighth IAS Annual Meeting*, Oct. 1993, vol. 2, pp. 1169–75.
- [8] C. R. Sullivan, "Optimal choice for number of strands in a litz-wire transformer winding", *IEEE Transactions on Power Electronics*, vol. 14, no. 2, pp. 283–291, 1999.
- [9] The MathWorks, Inc., <http://www.mathworks.com>, *MATLAB Version 6*, 2000.
- [10] C.R. Sullivan, T. Abdallah, and T. Fujiwara, "Optimization of a flyback transformer winding considering two-dimensional field effects, cost and loss", in *Proceedings of 16th Annual Applied Power Electronics Conference - APEC 2001*, 2001, pp. 116–22 vol.1.
- [11] C. R. Sullivan, "Computationally efficient winding loss calculation with multiple windings, arbitrary waveforms, and two- or three-dimensional field geometry", *IEEE Transactions on Power Electronics*, vol. 16, no. 1, pp. 142–150, Jan. 2001.
- [12] J. H. Spreen, "Electrical terminal representation of conductor loss in transformers", *IEEE Transactions on Power Electronics*, vol. 5, no. 4, pp. 424–9, 1990.
- [13] S. Crepez, "Eddy-current losses in rectifier transformers", *IEEE Transactions on Power Apparatus and Systems*, vol. PAS-89, no. 7, pp. 1651–1662, 1970.
- [14] P. N. Murgatroyd, "The toroidal cage coil", *IEE Proceedings, Part B*, vol. 127, no. 4, pp. 207–214, 1980.
- [15] W.G. Hurley, E. Gath, and J.G. Breslin, "Optimizing the ac resistance of multilayer transformer windings with arbitrary current waveforms", *IEEE Transactions on Power Electronics*, vol. 15, no. 2, pp. 369–76, Mar. 2000.
- [16] R. W. Erickson and D. Maksimovic, *Fundamentals of Power Electronics*, Kluwer Academic Publishers, second edition, 2001.
- [17] P.J. Lawrenson K.J. Binns and C.W. Trowbridge, *The analytical and numerical solution of electric and magnetic fields*, J. Wiley, 1992.
- [18] J. A. Ferreira, *Electromagnetic Modelling of Power Electronic Converters*, Kluwer Academic Publishers, 1989.
- [19] Jiankun Hu and C. R. Sullivan, "Optimization of shapes for round-wire high-frequency gapped-inductor windings", in *Proceedings of the 1998 IEEE Industry Applications Society Annual Meeting*, 1998, pp. 900–906.
- [20] J.D. Lavers and E.D. Lavers, "An accuracy assessment of 2-d vs. 3-d finite element models for ferrite core, sheet wound transformers", in *IEEE Applied Power Electronics Conference*, 2002, pp. 158–64 vol.1.
- [21] A.F. Hoke and C.R. Sullivan, "An improved two-dimensional numerical modeling method for e-core transformers", in *IEEE Applied Power Electronics Conference*, 2002, pp. 151–7 vol.1.
- [22] *Dartmouth Magnetic Component Research Web Site*, <http://engineering.dartmouth.edu/inductor>.
- [23] E. C. Snelling, *Soft Ferrites, Properties and Applications*, Butterworths, second edition, 1988.
- [24] The MathWorks, Inc., <http://www.mathworks.com>, *MATLAB Web Server 1.2.1*, 2000.